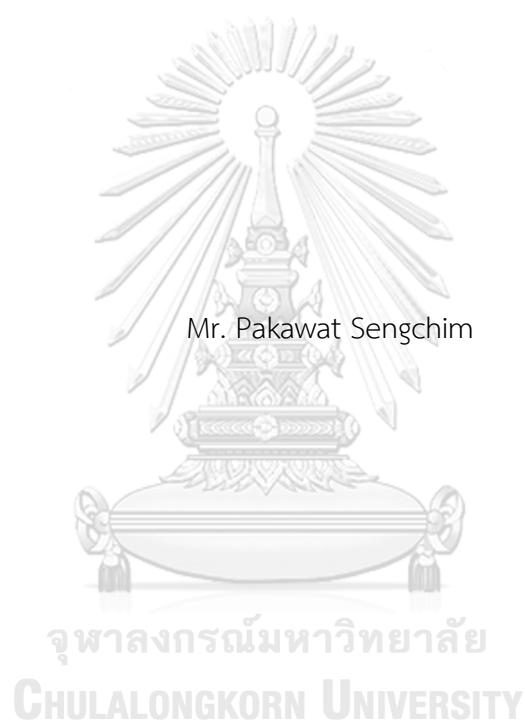


Electrochemical tubular fixed-bed reactor for conversion of pressurized CO₂ to CO



A Thesis Submitted in Partial Fulfillment of the Requirements
for the Degree of Master of Engineering in Chemical Engineering

Department of Chemical Engineering

FACULTY OF ENGINEERING

Chulalongkorn University

Academic Year 2021

Copyright of Chulalongkorn University

เครื่องปฏิกรณ์เคมีไฟฟ้าแบบท่อเบตนึ่งสำหรับการเปลี่ยนคาร์บอนไดออกไซด์ความดันสูงเป็น
คาร์บอนมอนอกไซด์



วิทยานิพนธ์นี้เป็นส่วนหนึ่งของการศึกษาตามหลักสูตรปริญญาวิศวกรรมศาสตรมหาบัณฑิต
สาขาวิชาวิศวกรรมเคมี ภาควิชาวิศวกรรมเคมี
คณะวิศวกรรมศาสตร์ จุฬาลงกรณ์มหาวิทยาลัย
ปีการศึกษา 2564
ลิขสิทธิ์ของจุฬาลงกรณ์มหาวิทยาลัย

ภควัฒน์ เชนงิม : เครื่องปฏิกรณ์เคมีไฟฟ้าแบบท่อเบตนิ่งสำหรับการเปลี่ยน
คาร์บอนไดออกไซด์ความดันสูงเป็นคาร์บอนมอนอกไซด์. (Electrochemical tubular
fixed-bed reactor for conversion of pressurized CO₂ to CO) อ.ที่ปรึกษาหลัก :
ผศ. ดร.พลัง บำรุงสกุลสวัสดิ์

ปฏิกิริยาการลดคาร์บอนไดออกไซด์ถูกใช้ในการกระตุ้นการเปลี่ยนคาร์บอนไดออกไซด์
เป็นคาร์บอนมอนอกไซด์ โดยปกติกระบวนการนี้จะศึกษาในสารละลายอิมิตัวด้วย
คาร์บอนไดออกไซด์ที่สถานะของเหลวโดยที่ความสามารถในการละลายของคาร์บอนไดออกไซด์ใน
น้ำมีค่าที่ต่ำมาก (0.033 โมลาร์) ที่ความดัน 1 บาร์และที่อุณหภูมิห้อง ส่งผลต่ออัตราการ
เกิดปฏิกิริยาและการถ่ายโอนมวล ในงานวิจัยนี้ได้ศึกษาเครื่องปฏิกรณ์เคมีไฟฟ้าแบบท่อเบตนิ่ง
สำหรับปฏิกิริยาการเปลี่ยนคาร์บอนไดออกไซด์เป็นคาร์บอนมอนอกไซด์โดยมีการออกแบบจะ
คำนึงถึงการขยายขนาดได้ง่ายและเครื่องปฏิกรณ์ประกอบด้วยเซลล์เคมีไฟฟ้าหลายเซลล์ที่สามารถ
ต่อกันเป็นแบบอนุกรมได้ โดยแต่ละเซลล์ประกอบไปด้วย 3 ส่วนหลัก คือ แอโนด, อิเล็กโทรไลต์
แข็ง และแคโทด นอกจากนี้โลหะซิงค์ถูกนำมาใช้เป็นตัวเร่งปฏิกิริยาเคมีไฟฟ้าสำหรับการเปลี่ยน
คาร์บอนไดออกไซด์เป็นคาร์บอนมอนอกไซด์ โดยที่มิน้ำไหลผ่านเซลล์เพื่อรักษาค่าการนำไฟฟ้า
ของอิเล็กโทรไลต์และเพื่อรักษาปฏิกิริยาไฟฟ้าเคมี การศึกษาผลกระทบของความดัน อัตราการไหล
และความต่างศักย์ที่ให้แก่ระบบที่มีผลต่ออัตราการเกิดปฏิกิริยาและผลผลิต จากการทดลองที่ความ
ดัน 10 บาร์ อัตราการไหลที่ 60 มิลลิลิตรต่อนาทีและความต่างศักย์ 7 โวลต์ ค่าความเข้มข้นของ
คาร์บอนมอนอกไซด์ได้ 1272 ส่วนในล้านส่วนและประสิทธิภาพของฟาราเดย์สูงที่สุดอยู่ที่ 19.61
เปอร์เซ็นต์

จุฬาลงกรณ์มหาวิทยาลัย
CHULALONGKORN UNIVERSITY

สาขาวิชา วิศวกรรมเคมี
ปีการศึกษา 2564

ลายมือชื่อนิสิต
ลายมือชื่อ อ.ที่ปรึกษาหลัก

6370219121 : MAJOR CHEMICAL ENGINEERING

KEYWORD: Electrochemical CO₂ reduction, Electrochemical tubular reactor, CO,
Pressure

Pakawat Sengchim : Electrochemical tubular fixed-bed reactor for conversion of pressurized CO₂ to CO. Advisor: Asst. Prof. PALANG BUMROONGSAKULSAWAT, Ph.D.

Electrochemical CO₂ reduction reaction (CO₂RR) can be used for activating the stable CO₂ molecule to the more active CO for downstream purposes. Usually, this process is carried out in CO₂-saturated aqueous solutions. The low solubility of CO₂ in water of 0.033 M at 1 bar of CO₂ and room temperature hinders both kinetics and mass transfer. In this study, a novel electrochemical tubular reactor for electrochemical CO₂RR is proposed. The design was made with ease of scale-up in mind. A reactor can contain multiple electrochemical cells connected in series. Each cell consists of 3 main parts: porous anode, porous solid electrolyte, and porous cathode, all of which allow bulk flow of gas streams through the tubular reactor. Zn is the active electrocatalyst at the cathode for the conversion of CO₂ to CO. Water is trickled through the cells to maintain electrolyte conductivity and also to sustain electrochemical reactions. The effects of CO₂ pressure and flow rate and applied voltage on the CO₂ conversion rate and yield are studied. About 1272 ppm of CO concentration and 19.61% of highest CO faradaic efficiency was obtained from a preliminary experiment conducted at 60 ml min⁻¹, 7 V of CO₂ at 10 bar.

Field of Study: Chemical Engineering

Student's Signature

Academic Year: 2021

Advisor's Signature

ACKNOWLEDGEMENTS

I am grateful to Assistant Professor Palang Bumroongsakulsawat, who gave the advice, counseling, assistance, and motivation for my thesis from the start of the first until the final semester. Besides, I am appreciative to Assistant Professor Apinun Soottitantawat, as the chairman, Assistant Professor Rungthiwa Methaapanon, and Dr. Pongkarn Chakthranont for their helpful advice and invaluable comment.

Moreover, I impress all my friends for giving me help and many valuable suggestions. Furthermore, I am thankful to the best partners, Momay and Tangkwa for their support in all things. Finally, I am also thankful to Chulalongkorn University and the technicians in the laboratory of the Center of Excellence on Catalysis and Catalytic Reaction Engineering (CECC), who provided the assistance.

Pakawat Sengchim

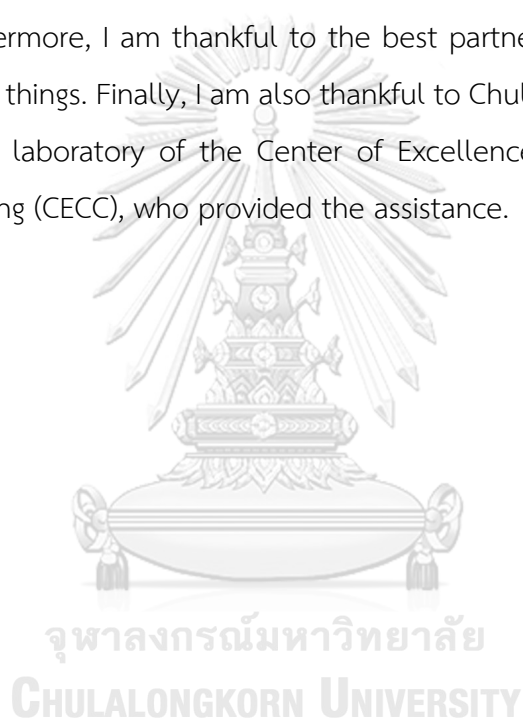


TABLE OF CONTENTS

	Page
ABSTRACT (THAI)	iii
ABSTRACT (ENGLISH)	iv
ACKNOWLEDGEMENTS	v
TABLE OF CONTENTS	vi
LIST OF TABLES	viii
LIST OF FIGURES.....	ix
CHAPTER 1 INTRODUCTION	1
1.1 Background	1
1.2 Objective	3
1.3 Scope of Study	3
1.4 Expected Benefits.....	3
1.5 Action Plan.....	4
CHAPTER 2 THEORY AND LITERATURE REVIEWS.....	5
2.1. Electrochemical CO ₂ reduction reaction	5
2.2. Faradaic Efficiency.....	9
2.3 CO ₂ in aqueous solution.....	10
2.4. Electrochemical of high pressurized CO ₂	10
2.5. Electrodeposition of Zn catalysts	15
CHAPTER 3 METHODOLOGY	19
3.1 Reactor Design.....	19
3.2 Experimental.....	20

3.2.1. Fabrication of Zn-deposit graphite felt as cathode	20
3.2.2. Electrochemical CO ₂ reduction	21
3.3 Characterization and Product Analysis.....	22
3.3.1. Characterization	22
3.3.2. Product analysis.....	22
CHAPTER 4 RESULTS AND DISCUSSION.....	23
4.1 CO ₂ reduction reaction	25
4.1.1 Voltage effect	26
4.1.2 Pressure effect.....	28
4.1.3 CO ₂ flow rate effect	31
4.2 Blank Test.....	34
CHAPTER 5 CONCLUSION AND SUGGESTIONS.....	35
5.1 Conclusions.....	35
5.2 Suggestions	36
REFERENCES.....	37
VITA	42

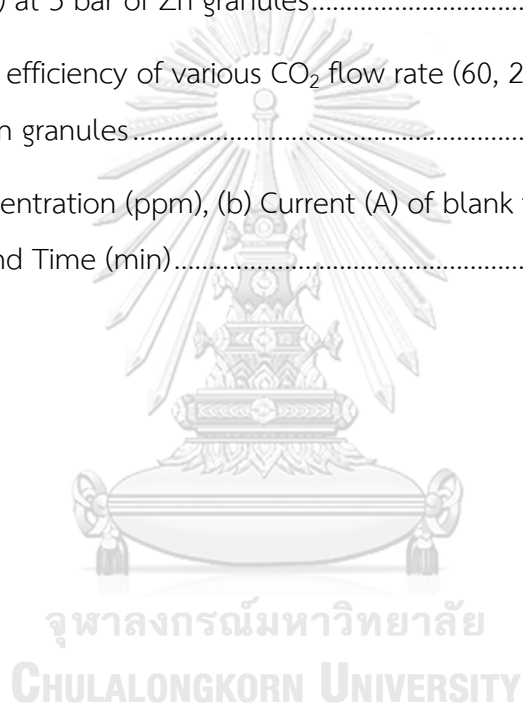
LIST OF TABLES

	Page
Table 1 Half-cell reaction pathways at cathode and anode in electrochemical CO ₂ reduction [9-12].....	6
Table 2 Effect of pressure on the product distribution of different metal electrodes in an electrochemical CO ₂ RR process [22].....	11
Table 3 Summary of CO ₂ RR to CO of Zn catalyst.....	16
Table 4 Summary of electrochemical CO ₂ RR in tubular fixed-bed reactor of Zn granules.....	25
Table 5 Summary of electrochemical CO ₂ RR in tubular fixed-bed reactor of Zn deposited on graphite felt.....	25

LIST OF FIGURES

	Page
Fig. 1 An outline of electrocatalysts for CO ₂ reduction [9].....	8
Fig. 2 Mechanism of electrochemical CO ₂ RR for produce CO ₂ to CO [19].....	9
Fig. 3 Effect of the pressure of CO ₂ on the current efficiency of CO at 12 mA/cm ² [6].	12
Fig. 4 Effect of pressure on CO ₂ RR at 300 mA/cm ² at various pressures and KOH concentrations [23].....	13
Fig. 5 Faradaic efficiencies of CO obtained at 45 °C [24].....	14
Fig. 6 Impact of pressure on faradaic efficiency of CO [18].....	15
Fig. 7 (a) CO faradaic efficiency for P-Zn and Zn foil and (b) Products distribution of P- Zn in an H-cell reactor [17].....	17
Fig. 8 Faradaic of CO at various constant potentials ranging from -0.6 to -1.1 V [28].	.18
Fig. 9 FEs of CO, H ₂ , and syngas and CO/H ₂ ratios for CO ₂ RR on Zn catalysts in CO ₂ - saturated 0.1 M KHCO ₃ at 40 °C with different potentials [7].....	19
Fig. 10 Electrochemical CO ₂ RR cell configuration.....	20
Fig. 11 Schematic of Fabrication of Zn-deposited on graphite felt as cathode.....	21
Fig. 12 Schematic of Electrochemical of high pressurized CO ₂	22
Fig. 13 SEM analysis of (a) Graphite felt , (b, c) Zn deposited on graphite felt, and (d) Zn granules.....	24
Fig. 14 (a) CO concentration (ppm), (b) current and Time (min) at 3 bar and CO ₂ flow rate 60 ml min ⁻¹ of Zn granules and Zn deposited.	28
Fig. 15 CO faradaic efficiency (%) and voltage (5-8 V) at 3 bar and CO ₂ flow rate 60 ml min ⁻¹ of (a) Zn granules, (b) Zn deposited on graphite felt.	28

Fig. 16 (a) CO concentration (ppm), (b) Current (A) and various pressure (bar) at 8V and CO ₂ flow rate 60 ml min ⁻¹ of Zn granules.....	30
Fig. 17 CO faradaic efficiency (%) and various pressure (bar) at 8V and CO ₂ flow rate 60 ml min ⁻¹ of Zn granules and Zn deposited.....	30
Fig. 18 (a) CO faradaic efficiency (%), (b) Current and voltage (5-8 V) at 1.5, 3, 8, 10 bar and CO ₂ flow rate 60 ml min ⁻¹ of Zn granules.....	31
Fig. 19 (a) CO concentration, (b) Current of various CO ₂ flow rate (60, 200 ml min ⁻¹) and Voltage (5-8 V) at 3 bar of Zn granules.....	33
Fig. 20 CO faradaic efficiency of various CO ₂ flow rate (60, 200 ml min ⁻¹) and Time (min) at 3 bar of Zn granules.....	34
Fig. 21 (a) CO concentration (ppm), (b) Current (A) of blank test comparing at 3 bar, 5-8 V, 60 ml min ⁻¹ and Time (min).....	35



CHAPTER 1

INTRODUCTION

1.1 Background

Nowadays, the concentration of greenhouse gases in the atmosphere is increasing. The main part is carbon dioxide (CO_2), which is strongly linked to global warming and climate change issues. As a potential solution to this challenge, CO_2 may be converted into valuable products via a carbon dioxide reduction reaction (CO_2RR) [1]. CO_2RR has been proposed as a promising method to combat rising carbon dioxide levels by converting CO_2 into renewable fuels or valuable chemicals. There are several other methods in CO_2 utilization, namely thermal catalysis, photochemical reduction, photoelectrochemical reduction, and enzymatic CO_2 conversion [1, 2]. In comparison with these methods, electrochemical CO_2RR is considered as one of the most useful techniques for the decarbonization process which utilizes clean energy sources and carry out at room temperature. Moreover, electrochemical CO_2RR can be obtained high CO selectivity [1, 3]. CO is an essential product because it is mainly used as a feedstock for the Fischer–Tropsch synthesis, methanol production, and pharmaceutical industry [4].

Generally, Electrochemical CO_2RR is challenging because the low solubility of CO_2 in aqueous electrolytes at ambient conditions hinders mass transfer of CO_2 [5]. An interesting strategy to reduce mass transfer limitation is the utilization of gas diffusion electrodes (GDE), and the process carried out at high pressure [6]. Zn catalysts are known to selectivity lead to the product of CO [7]. There are 2 main reactions, CO_2RR at the cathode and oxygen evolution reaction (OER) at the anode. The hydrogen

evolution reaction (HER) is competing with CO at the cathode. These reactions are presented in Eqs. (1)-(6).

Cathode reaction (CO₂RR)



Anode reaction (OER)



Overall reaction



In this study, a novel scalable electrochemical tubular fixed-bed reactor is developed for gas-phase CO₂ reduction to CO. It features only a single chamber; cathode and anode products are mixed as the reaction gas mixture flows along the reactor. Even though the generated mixture of CO and O₂ presents risk of explosion, this can be avoided by operating outside the flammability limits. For example, flue gas from an incinerator, which contains ca. 5 % CO₂ diluted in mostly N₂, may be suitable for this reactor. The reactor is made from stainless steel and reactor lining is 3D printed. Saturated CO₂ gas was fed through a porous cathode that consists of Zn catalyst deposited on a carbon support. The effects of CO₂ flow rates, pressure, and applied cell voltages on CO production rates and faradaic yields are studied.

1.2 Objective

To study the behavior of the novel electrochemical tubular fixed-bed reactor for electrochemical reduction of CO₂ to CO.

1.3 Scope of Study

1.3.1. Pressure applied to the reactor (1-10 bar)

1.3.2. Catalyst is Zinc granules and Zinc deposited on graphite felt

1.3.3. Reaction Conditions were applied voltage (5-8 V), CO₂ flow rate (60, 200 ml/min), and water is continuously trickled through the bed at 1 mL/min

1.3.4. anion exchange resin beads are used as the electrolyte in the cell.

1.4 Expected Benefits

1.4.1. To overcome the main hurdle of the CO₂ electrochemical conversion in aqueous solution, its low solubility, and to achieve good faradaic efficiency in CO.

1.4.2. To explore conditions for scale-up.

CHAPTER 2

THEORY AND LITERATURE REVIEWS

2.1. Electrochemical CO₂ reduction reaction

Electrochemical CO₂RR is considered as one of the most useful techniques for the decarbonization process into fuel and chemical products such as CO, CH₄, HCOOH, and some other products [1, 8]. The electrochemical CO₂RR occurs at the interface of electrode/electrolyte, which involves three main steps: (i) absorption of the CO₂ on the surface of the catalysts; (ii) transfer of at least two protons and electrons to break one of the oxygen-carbon bonds forming a water molecule in the case of CO or subsequent further protonation; (iii) desorption of the final products from the electrode surface [1, 9]. However, CO₂RR occurs to need a large negative potential and the E₀ value of hydrogen evolution reaction (HER) derived from hydrolysis of water is relatively positive compared to other C1 products. Then, HER becomes the main competitive reaction of CO₂RR [9]. Due to this, the CO₂RR for converting CO₂ into CO, the reaction $\text{CO}_2(\text{g}) \rightarrow \text{CO}(\text{g}) + \frac{1}{2} \text{O}_2(\text{g})$ has an E⁰ value of -1.334 V vs SHE, indicating that it is a non-spontaneous reaction. As a result, this cell requires a voltage greater than the equilibrium electrode potential same as the electrolytic cell. When a cell receives an electrical current from an applied voltage, the electron can transfer from the anode to the cathode, provided that the electron transfers in the system according to the Faraday's law because the electric current that flows through an electrochemical cell is related to the moles of electrons and subsequently occur the CO₂RR.

The cell of electrochemical CO₂RR consists of cathode and anode in which CO₂ was continuously fed and applied voltage. At the cathode, there was a CO₂RR and HER

and at the anode, there was an oxygen evolution reaction (OER) from water is oxidized to molecular oxygen [9, 10]. According to the thermodynamic theory, the minimum potential required for a CO₂RR is the half-cell standard potential described by $E^0 = -\Delta G^0/nF$, where $-\Delta G^0$ is the Gibbs free energy at 1 atm and 298 K, n is the number of moles of electrons transferred in the half-cell reaction, and F is faraday constant (96485 C/mol) [11]. For conversion of CO₂ to CO, the half-cell reaction $\text{CO}_2(\text{g}) + 2\text{H}^+(\text{aq}) + 2\text{e}^- \rightarrow \text{CO}(\text{g}) + \text{H}_2\text{O}(\text{l})$ with $\Delta G^0 = 20.09$ kJ/mol has $E^0 = -0.104$ V vs SHE. Other half-cell standard potentials are shown in Table. 1.

Table 1 Half-cell reaction pathways at cathode and anode in electrochemical CO₂ reduction [9-12]

Electrode	Half-Electrochemical Reactions	E_0 (V vs SHE)
Cathode reaction (CO ₂ RR)	$\text{CO}_2 + 2\text{H}^+ + 2\text{e}^- \rightarrow \text{CO} + \text{H}_2\text{O}$	-0.104
	$\text{CO}_2 + 2\text{H}^+ + 2\text{e}^- \rightarrow \text{HCOOH}$	-0.250
	$\text{CO}_2 + 6\text{H}^+ + 6\text{e}^- \rightarrow \text{CH}_3\text{OH} + \text{H}_2\text{O}$	+0.016
	$\text{CO}_2 + 8\text{H}^+ + 8\text{e}^- \rightarrow \text{CH}_4 + 2\text{H}_2\text{O}$	+0.169
	$2\text{CO}_2 + 12\text{H}^+ + 12\text{e}^- \rightarrow \text{C}_2\text{H}_4 + 4\text{H}_2\text{O}$	+0.064
(HER)	$2\text{H}^+ + 2\text{e}^- \rightarrow \text{H}_2$	0.000
Anode reaction (OER)	$2\text{H}_2\text{O} \rightarrow \text{O}_2 + 4\text{H}^+ + 4\text{e}^-$	+1.230

However, the applied voltage affects to consumes CO₂ concentration at the electrode surface, the overall reaction rate can be limited by the rates of CO₂ transfer.

Moreover, according to the Nernst equation, the change in concentration affects the equilibrium electrode potential and this effect can be approximated by the concentration overpotential as the equation (6). Thus, the electrochemical cell improves the minimum energy requirements for CO₂RR [11, 13] which the Nernst equation gives the relationship between the equilibrium electrode potential and the concentration or partial pressure. The Nernst equation for conversion CO₂ to CO as shown in equation (6) [14].

$$E^0 = \frac{\Delta G_f}{nF} - \frac{RT}{nF} \ln \frac{p_{CO_2}}{p_{CO} \sqrt{p_{O_2}}} \quad (6)$$

Where ΔG_f is the Gibbs free energy of formation, R is the gas constant, T is the absolute temperature, n is the moles of electrons transferred in the reaction, F is Faraday's constant, p_{CO_2} is the partial pressure of CO₂, p_{CO} is the partial pressure of CO, and p_{O_2} is the partial pressure of O₂.

Furthermore, the difference between the electrode potential and the equilibrium electrode potential is referred to the reaction rate or the electron transfer rate. The kinetics of the electrochemical cell depends on the electrode potential and the equilibrium electrode potential. According to the Butler-Volmer equation as equation (7), increasing the electrode potential affects the electrical current with the exponential relationship [15]. Suppose the electrical current is increased following the cell voltage. It means the electron transfer rate in the electrochemical cell same increased.

$$j = j_0 \{ \exp[-\alpha F \eta / RT] - \exp[(1 - \alpha) F \eta / RT] \} \quad (7)$$

Where j is the electrode current density, j_0 is the exchange current density, α is the charge transfer coefficient dimensionless, F is Faraday's constant, η is the activation overpotential defined as the difference between the electrode potential

and the equilibrium electrode potential, R is the gas constant, and T is the absolute temperature.

A CO_2 reduction electrocatalyst that can selectively produce desired chemicals while suppressing undesired side reactions is essential to achieve a highly efficient system [6, 16]. Many researchers have investigated the selectivity of products with various metals at the cathode side such as Pd, Ag, Zn, Cu, Sn, Ru, Pt, Ni. Based on the primary CO_2 reduction product, CO selective metals (e.g., Au, Ag, and Zn), formic acid selective metals (e.g., Sn, In, and Pb), and hydrogen-selective metals (e.g., Fe, Ni, and Pt). [16, 17] as shown in Fig. 1.

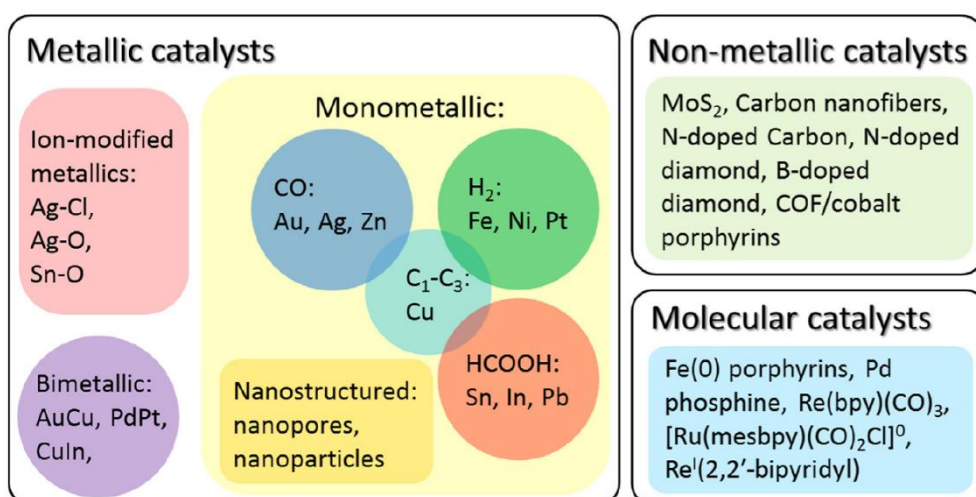


Fig. 1 An outline of electrocatalysts for CO_2 reduction [9].

A key challenge of electrochemical CO_2 RR is the preparation of catalysts with high activity, selectivity, and stability [5, 16]. Au and Ag are known as the best metal catalysts for conversion CO_2 to CO with high activity and selectivity. However, it is

difficult to use on a large scale in industrialization, due to the high price and scarce reserve of precious metals [5]. Zn, as an earth-abundant metal, is one of the choices to use as a catalyst to produce CO but with relatively lower activity and CO selectivity than Au and Au. To improve the activity and selectivity of Zn catalysts, many alternatives have been used in the preparation of catalysts such as electrodeposition, anodization, oxide reduction [5, 16, 17].

The mechanism of electrochemical CO₂RR for produce CO₂ to CO. At the beginning, CO₂ and HCO₃⁻ are absorbed on the surface of the electrode. Subsequently, (1) CO₂ is reduced to CO₂^{*} by one electron from electrochemical process; (2) the CO₂^{*} is electrochemically reduced to the reaction intermediate of COOH^{*}; (3) the COOH^{*} is reduced with an electron and a proton to CO^{*} that desorbs from Zn to produce the CO gas [18].

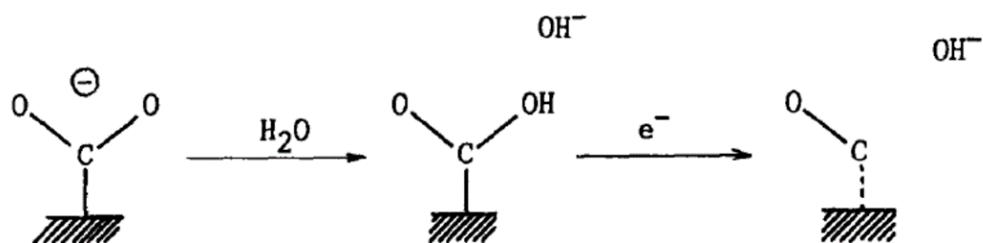


Fig. 2 Mechanism of electrochemical CO₂RR for produce CO₂ to CO [19]

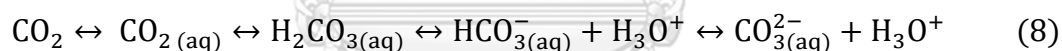
2.2. Faradaic Efficiency

Faradaic efficiency (FE) is the parameter of the desired product. It is defined as the electric charge used for the formation of the desired product over the total charge passed between the electrodes. The faradaic efficiency represents the selectivity toward a specific product, thus an improvement on the FE can directly increase the

amount of CO₂ converted to the desired product, reduce product separation cost, and lower the energy penalty of the electrocatalysis.

2.3 CO₂ in aqueous solution

Carbon dioxide dissolves in water leading to the formation of CO₂ species such as carbonic acid (H₂CO₃), bicarbonate (HCO₃⁻), and carbonate (CO₃²⁻). The equilibrium concentration of these species is a function of the partial pressure of CO₂ and the pH. Under ambient pressure, the solubility of CO₂ in water is about 0.034 mol/L and pH = 3.9. The equation (8) shows that introducing CO₂ in an aqueous solution leads to a complex series of reversible reactions between CO₂ species. In the solution with a pH up to about 6, CO₂ is in the form of a weak carboxylic acid; at pH between 6 and 10.3, HCO₃⁻ anions are formed; and at pH above 10.3, HCO₃⁻ deprotonates further to CO₃²⁻ [11]. Other approaches to increasing the solubility of CO₂ involved the use of high-pressure CO₂ or the use of non-aqueous solvent [20].



2.4. Electrochemical of high pressurized CO₂

In aqueous solvents, the hydrogen evolution reaction (HER) is a competitive reaction with CO₂ reduction reaction (CO₂RR) because the solubility of CO₂ in water at ambient pressure is low which indicate mass transfer limitations [21]. One strategy to overcome this limitation, the partial pressure of CO₂ in the gas fed into the electrolyzer impacts the rate of CO₂ mass transfer to the electrode surface due CO₂ solvent solubility relationship [11]. However, the high-pressure CO₂RR requires balancing the

pressure in the anode and cathode chambers to prevent damage to the separator [6, 21].

Hara et al. (1995) [22] studies the electrochemical reduction of CO₂ at high pressure (30 atm) in an aqueous KHCO₃ solution. The electrolysis cell was carried out in a glass cell in a stainless-steel autoclave. The catholyte and anolyte compartments were separated by a Nafion 417 sheet. The electrolyte was deaerated by bubbling CO₂ for 30 min, a known pressure of CO₂ was introduced into the electrolysis cell. In the Zn electrode under a CO₂ pressure of 30 atm at a current density of 163 mA/cm², CO with faradaic efficiencies of 49%.

In Table. 2, summarizes a typical example report of CO₂ pressure (1, 30 atm) on product selectivity over different metal electrodes by Hara et al. For group C, catalysts like Ag, Zn, and Sn, did not report a major shift in the type of CO₂RR products at higher pressure but the faradaic efficiency towards CO and HCOOH did increase which was affected to increased CO₂ solubility at high pressure [11, 19].

Table 2 Effect of pressure on the product distribution of different metal electrodes in an electrochemical CO₂RR process [22]

Effect of pressure			
Group	Cathode catalyst	Major products at	
		1 atm	30 atm
A	Ti, Nb, Ta, Mo, Mn, Al	H ₂	H ₂
B	Zr, Cr, W, Fe, Rh, Ni, Pd, Pt, Si	H ₂	CO and HCOOH

C	Ag, Au, Zn, In, Sn, Pb, Bi	CO and HCOOH	CO and HCOOH
D	Cu	CH ₄ and C ₂ H ₆	CO and HCOOH

In the undivided cell. Proietto et al. (2021) [6] studies the electrochemical reduction of pressurized CO₂ to overcome the low solubility of CO₂ in an aqueous solution and achieve good faradaic efficiency. The electrolysis was performed in CO₂ saturated water solution of 0.2 K₂SO₄ at a silver plate cathode. In this report when the pressure was increased, could lead to a strong enhancement of the CO production. In the same way, the best faradaic efficiency of CO was 67% (30 bar) at 12 mA/cm² as shown in Fig. 2. They explain the enhancement of the CO₂ concentration in the bulk is effective to assist the electrocatalytic properties of CO generation.

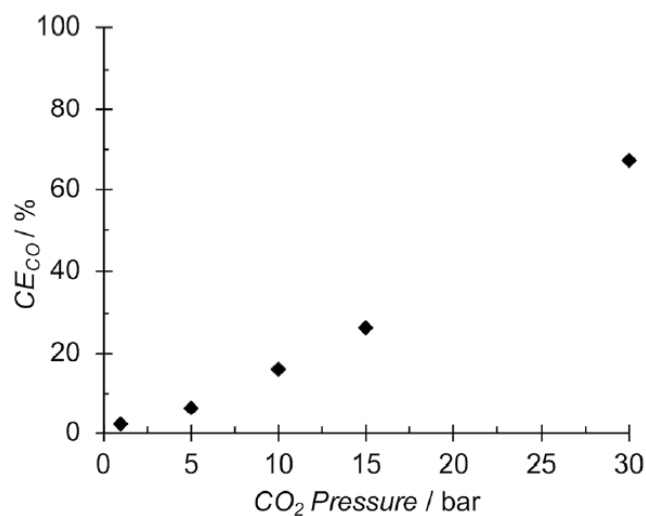


Fig. 3 Effect of the pressure of CO₂ on the current efficiency of CO at 12 mA/cm² [6].

Gabardo et al. (2018) [23] studies to boost the performance of the electrochemical reduction of CO₂ with high alkalinity electrolytes to reduce the

overpotentials needed to generate CO from CO₂ on a silver catalyst. However, these conditions have detrimental effects on product selectivity, increasing the production of formic acid. Therefore, the electrolyzers will need to operate at higher pressure together with high alkalinity electrolytes to achieve the problem. As they hypothesized that an increased concentration of CO₂ on the surface catalyst due to the increase in pressure could lead to increase CO faradaic efficiency and the reaction switching from formic acid to CO and reduce the factors of forming formic acid. From the results in 10 M KOH, the faradaic efficiency of CO increased from 42% (1 atm) to 85% (7 atm) at the current density of 300 mA/cm². However, the faradaic efficiency of formic acid decreased from 38.2% (1 atm) to 12% (7 atm) as shown in Fig. 3.

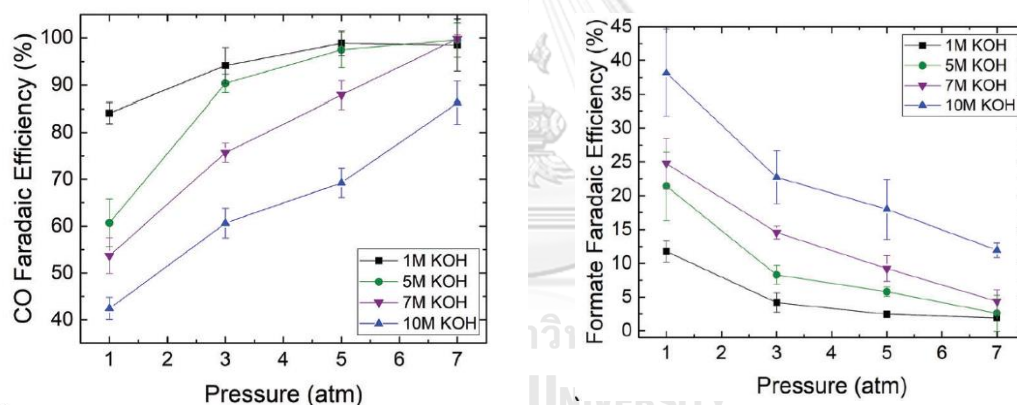


Fig. 4 Effect of pressure on CO₂RR at 300 mA/cm² at various pressures and KOH concentrations [23].

In the membrane electrode assembly (MEA). Messias et al. (2019) [24] The main objective of this study was to investigate the effect of pressure and the scalability of the process. They have used an inexpensive commercial foil of the common metal zinc as an electrocatalyst. The reactor was operated at 45°C which faradaic efficiency

of CO from 62% at 10 bar to 82% at 30 bar as shown in Fig. 4. The cell potentials of electrolysis carried out in semi-continuous mode were in the range of -3.5 V to -3.9 V vs Ag/Ag⁺ QRE. A flow rate of electrolyte at 1 ml/min containing 90 wt% H₂O and EMIMOTf. The effect of pressure at 30 bar shows a significant influence on CO selectivity and CO productivities. From in Fig. 5 at 10 bar, observe that CO production is higher and presents a maximum at a flow rate of 2.5 ml min⁻¹. However, increasing the CO flow rate causes a decrease in the residence time of CO₂ at the electrode surface, influencing the H₂/CO ratio.

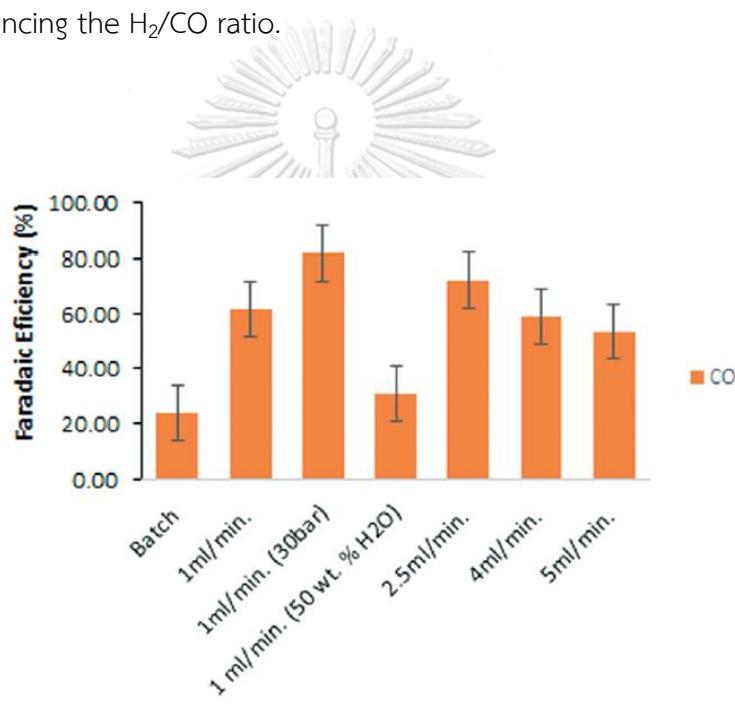


Fig. 5 Faradaic efficiencies of CO obtained at 45 °C [24]

Meanwhile, Dufek and co-workers (2012) [18]. use Ag-based gas diffusion electrode (Ag GDE) and pressurized CO₂ to address CO₂ reduction is hindered by poor kinetics and limited CO₂ solubility in aqueous solution. The advantage of performing the reduction at high pressure is increasing the pressure increases the solubility of CO₂ according to Henry's law. From the result, they have shown an increase in the faradaic

efficiency for CO generation occurred as the pressure was increased from ambient. At pressures above 15 atm, the faradaic efficiency of CO generation was above 80% at 225 mA/cm² and 60 °C. as shown in Fig. 5. In the pressurized cell, the determination of the faradaic efficiency (FE) is complicated by residence time of gases in the system due to the lag time. Thus, elevating flow rate of CO₂ were operated to more effectively sweep product gases from the pressurized electrolysis system and to more readily follow the real-time cell performance.

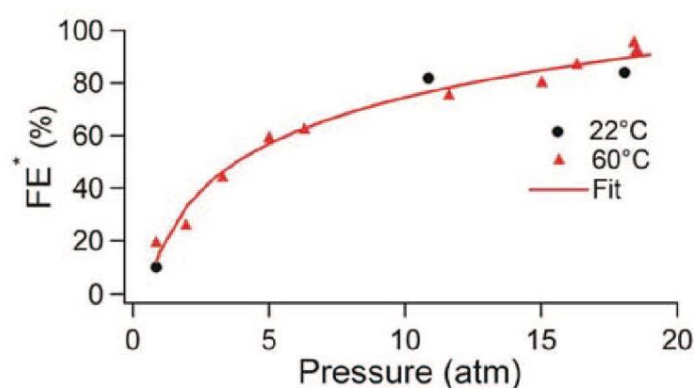


Fig. 6 Impact of pressure on faradaic efficiency of CO [18]

2.5. Electrodeposition of Zn catalysts

The non-noble metal Zn is one of the promising materials because of its abundant reserves and particularly selective production of CO, but the Zn metal reduces CO₂ to CO with low activity and CO selectivity than the noble metal Au and Ag catalyst [17]. To overcome this limitation, efforts have been made to increase the active surface area of a Zn electrocatalyst and allow a much higher CO selectivity [16].

In this report, develop the Zn electrode with the electrodeposition to study the behavior of the tubular reactor. The electrodeposition process is metallic coating onto the porous support (base material), which occurs through the electrochemical reduction of metal ions from an electrolyte. The electrodeposition process consists of the object to be coated or called cathode, electrolyte, anode, and the power supply to make the current flow [25].

Table 3 Summary of CO₂RR to CO of Zn catalyst

Researcher	Catalyst	Experimental Condition	CO Faradaic Efficiency
Wen Luo, et al. (2019) [17]	Zn foil	H-cell 0.1 M KHCO ₃ -0.95 V vs RHE	50%
	Porous Zn (P-Zn)	H-cell 0.1 M KHCO ₃ -0.95 V vs RHE	95%
Lu, Y. et al. (2018) [26]	ED Zn	H-cell 0.5 M KHCO ₃ -1.1 V vs RHE	80%
Jonathan Rosen, et al. (2015) [27]	Electrodeposited Zn dendrites	H-cell 0.5 M NaHCO ₃ -1.1 V vs RHE	79%
Da Hye Won, et al. (2016) [28]	Hexagonal Zn	H-cell 0.5 M KHCO ₃ -0.95 V vs RHE	85.4%
Bin hao Qin, et al. (2018) [7]	Electrodeposited Zn catalyst on Cu foam	H-cell 0.1 M KHCO ₃ -0.9 V vs RHE	85%

In an H-cell reactor. Luo et al. (2019) [17] Zn electrocatalyst is synthesized using an electrochemical method to boost the performance of CO₂RR with electrodeposition method to prepare porous Zn catalyst (P-Zn); that is, the sample deposition of Zn onto the Cu mesh. Interesting this report is the enhanced CO₂ reduction performance of the P-Zn in selectivity compare with Zn foil. From the results, porous Zn catalyst can convert CO₂ to CO at high faradaic efficiency (FE_{CO}, ~95%), compared with that of Zn foil (FE_{CO}, =50%) as shown in Fig. 7a. Because the Cu mesh used as support played the role in increasing the surface area of P-Zn, and the difference mainly corresponds to lower FEs for H₂ on P-Zn as shown in Fig 7b.

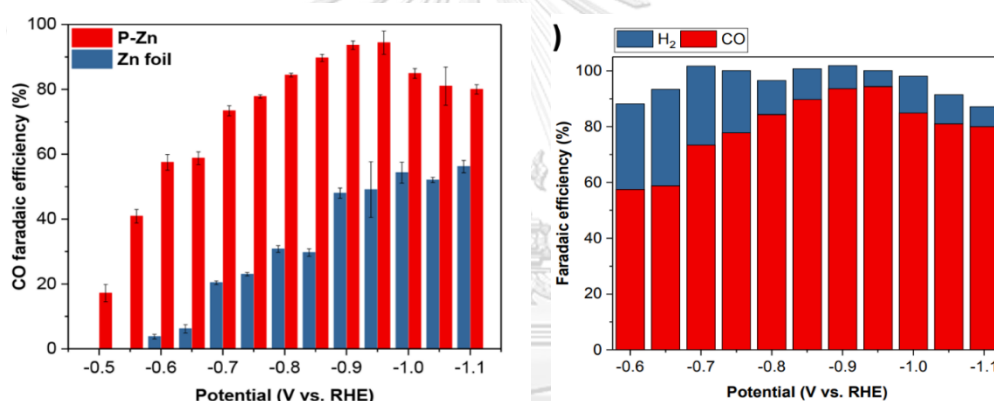


Fig. 7 (a) CO faradaic efficiency for P-Zn and Zn foil and (b) Products distribution of P-Zn in an H-cell reactor [17].

Luo et al. (2018) [29] studies the ZnO catalysts were synthesized on Zn foil substrates using various preparation methods, containing hydrothermal, spray-coating, and electrodeposition methods. The result found that ZnO catalysts with different morphologies, are nanowires, nanoparticles, and nanoflowers form respectively. Then, the synthesized ZnO catalysts were electrochemically reduced at -1.6 V versus reversible hydrogen electrode (RHE) cause a porous morphology composed of thin hexagonal flakes, which exhibited a higher surface area. The CO₂RR performances of this catalysts were evaluated in H-cell with CO₂-saturated 0.1 KHCO₃ as the electrolyte.

It shows that all three catalysts are highly selective towards CO with exceeding 90% FE at moderate overpotentials.

Won et al. (2016) [28] have reported that a hexagonal Zn catalyst that was electrodeposited on a Zn foil had good selectivity of CO. They prepare the hexagonal Zn catalyst by electrodeposition of ZnCl_2 on Zn foil. The CO_2 RR performances were carried out at potential range from -0.6 to -1.1 V (vs RHE) in a CO_2 -saturated 0.5M KHCO_3 electrolyte. The highest FE for CO was 85.4% at -0.95 V on the hexagonal Zn, which compared with Zn foil was 25.1% of FE for CO as shown in Fig. 8. In summary, they found that development of the hexagonal Zn catalyst was high selectivity towards CO. In particular, DFT calculations demonstrated that (101) facet is appropriate to CO production due to its lower reduction potential for CO_2 reduction to CO and higher energy barrier for HER.

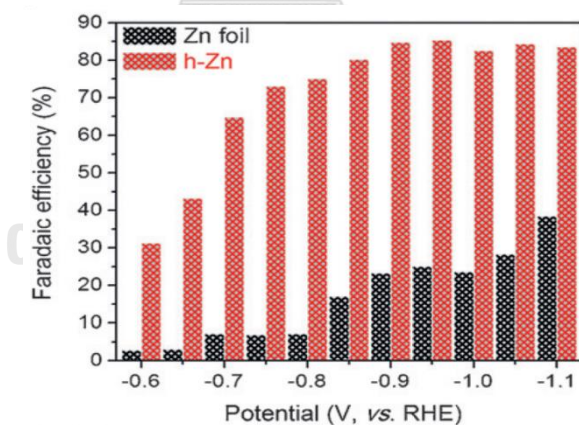


Fig. 8 Faradaic of CO at various constant potentials ranging from -0.6 to -1.1 V [28].

Qin et al. (2018) [7] studies Zn catalysts have been prepared on electrochemically polished Cu foam by the electrochemical deposition method. For electrocatalytic test for CO₂RR performances was conducted in an airtight H-cell. the Faradaic efficiency (FE) of CO₂RR to syngas is greater than 85% at -0.9V vs RHE in aqueous solution.

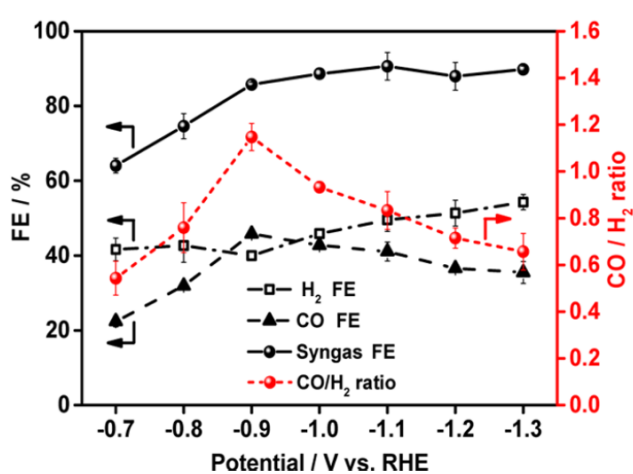


Fig. 9 FEs of CO, H₂, and syngas and CO/H₂ ratios for CO₂RR on Zn catalysts in CO₂-saturated 0.1 M KHCO₃ at 40 °C with different potentials [7].

CHAPTER 3

METHODOLOGY

3.1 Reactor Design

The reactor was made from stainless steel. A reactor lining made by 3D printing was inserted inside the reactor to prevent a short circuit. In Fig. 10 displays the configuration details and the 14 mm cell diameter. There are three main parts in the cell. First, the porous cathode is zinc granules (Sigma-Aldrich) or zinc deposited on graphite felt as a cathode for converting CO₂ to CO that formed at a thickness of 3 mm. Second, the porous solid electrolyte is formed from a 2 mm thick bed of anion-

exchange resin beads (Amberlite IRA402 Chloride form) for ionic conductivity and separation of the electrodes and the anode is platinized titanium mesh (Fuel Cell Store). Finally, graphite felt is used to provide compression for firm electrical contacts between cell components.



Fig. 10 Electrochemical CO₂RR cell configuration

3.2 Experimental

This work consists of 2 parts: electrochemical conversion of pressurized CO₂ with Zn granule cathodes and Zn graphite felt as cathodes.

3.2.1. Fabrication of Zn-deposit graphite felt as cathode

The cathode was prepared by the electrodeposition method at room temperature and atmospheric pressure. Graphite felt (diameter 14 mm) is used to support which high porosity, high conductivity, and high surface area for disperse gas. A titanium plate was used as the working electrode and the counter electrode in the electrodeposition process, respectively. This process uses 0.1M of ZnSO₄·7H₂O (Sigma-

Aldrich) 100 ml as an electrolyte and deposition at a constant 10 mA for 30 mins, as presented in Fig 11.

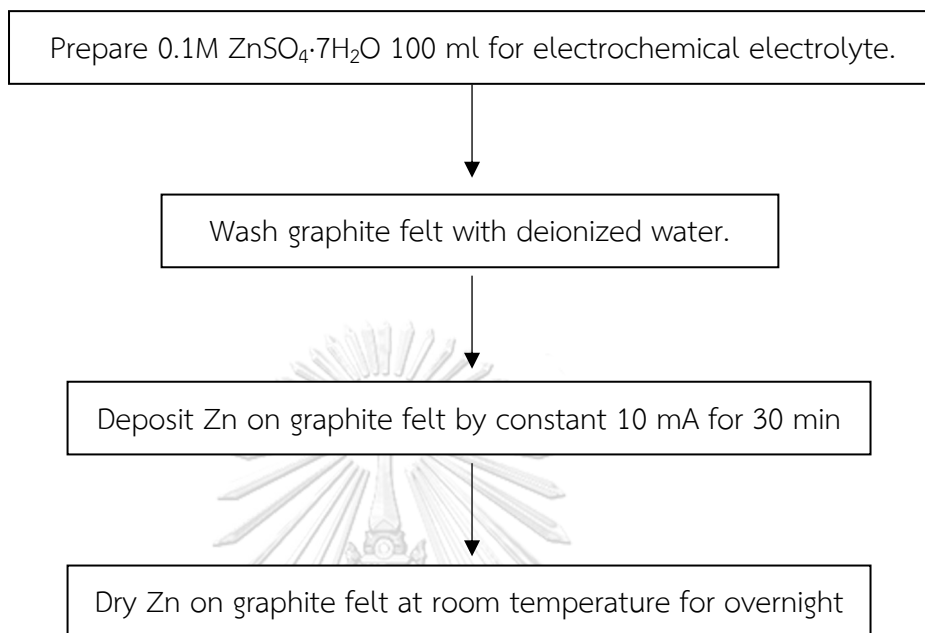


Fig. 11 Schematic of Fabrication of Zn-deposited on graphite felt as cathode

3.2.2. Electrochemical CO₂ reduction

Gas mixtures containing CO₂ are fed continuously to the tubular reactor. The flow rate is controlled by a mass flow controller. Potentiostat galvanostat Autolab PGSTAT101 is used to apply cell voltages for electrochemical CO₂RR. Water is continuously trickled through the bed at 1 mL/min to sustain the ionic conductivity of the anion-exchange resin bed. Before the test, water was saturated with CO₂ by flowing CO₂ at desired pressure in the water drum overnight, and flowing CO₂ was maintained during the reaction. CO concentration was analyzed by Infrared Gas Analyzer (Model IR200, YOKOGAWA) in real-time as presented in Fig. 12. The effects of Pressure (1.5, 3, 8, and 10 bar), CO₂ flow rates (60 and 200 ml min⁻¹), and applied cell voltages (5, 6, 7, and 8 V) will be studied.

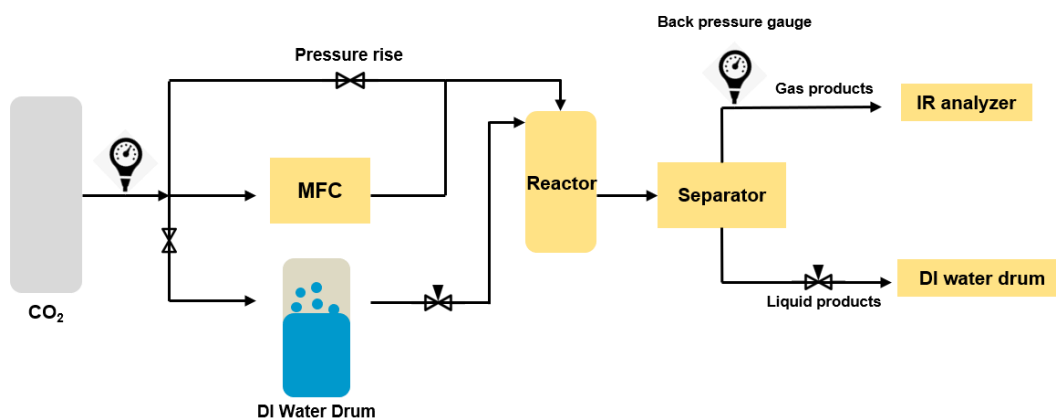


Fig. 12 Schematic of Electrochemical of high pressurized CO_2

3.3 Characterization and Product Analysis

3.3.1. Characterization

3.3.1.1 Scanning electron microscopy with Energy-dispersive X-Ray (SEM-EDX) is a technique that scans the surface with the electron beam. The electrons beam interacts with the sample and a number of signals are produced for detecting a surface of graphite felt. Furthermore, EDX could characterize and measure the elemental composition to confirm that Zn-metal can deposit on graphite felt with the electrodeposition method.

3.3.2. Product analysis

3.3.2.1 The Current from CO₂RR in an electrochemical tubular reactor could calculate Faradaic efficiency of CO product by Eqs. (9).

$$\begin{aligned} \text{FE}\% &= \frac{\text{Number of moles of electrons required for reducing CO}_2 \text{ to CO}}{\text{Total number of moles of electrons passed}} \\ &= \frac{y \int_0^t C_{\text{CO}} dt \times \text{flowrate} \times F}{\int_0^t I dt} \end{aligned} \quad (9)$$

When

y = Stoichiometric coefficient of electron in Eqs (1), which is 2.

C_{CO} = Concentration of CO produced at various times

F = Faraday constant

I = Electric current

t = Time



CHARTER 4
RESULTS AND DISCUSSION

จุฬาลงกรณ์มหาวิทยาลัย
CHULALONGKORN UNIVERSITY

The purpose of this work was to study the behavior of the novel electrochemical tubular fixed-bed reactor for electrochemical reduction of CO₂ to CO. The high pressure, applied voltage, and CO₂ flow rate are interesting parameters for preliminary electrochemical CO₂ reduction. In the experimental, the catalyst is Zn granule, and Zn-deposit on graphite felt. Fig. 13 shows the SEM image of Carbon felt, and Zn particles appeared on graphite felt.

The SEM morphology of graphite felt, a smooth carbon fiber with a diameter of 10 μm , is shown in Fig. 13a. After the electrodeposition, Zn was disorderly formed

on the carbon fiber with a diameter of about $\sim 10\ \mu\text{m}$ in Fig. 13b; however, Zn was only deposited on the surface and not inside the graphite felt, as can be seen from pure carbon fiber inside. Zn morphology on graphite felt is shown in Fig. 3c as hexagonal flakes. In Fig. 13d shows the SEM morphology of Zn granules with spherical, nonspherical shapes and rough surfaces with a diameter of $\sim 0.5\text{-}1\ \text{mm}$.

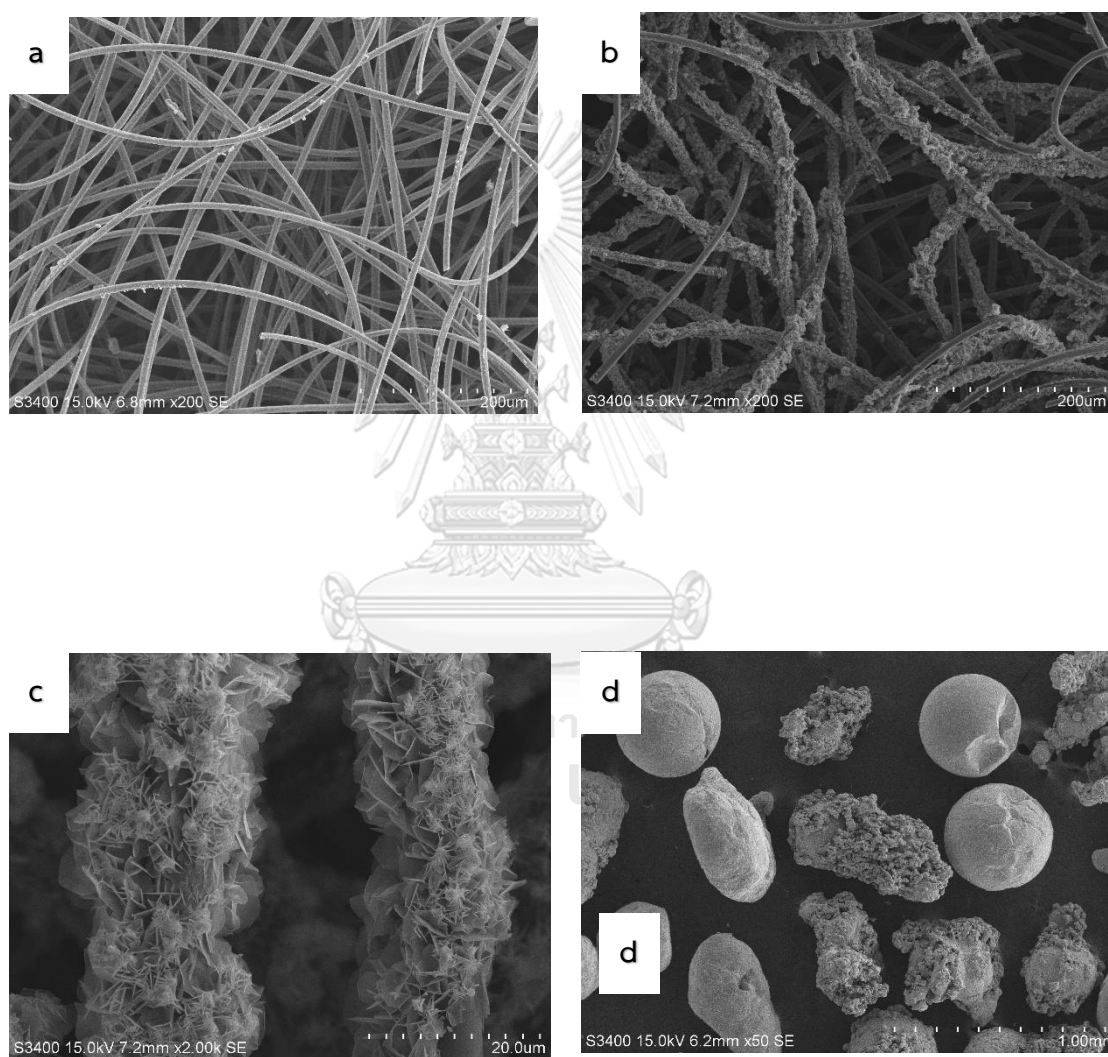


Fig. 13 SEM analysis of (a) Graphite felt , (b, c) Zn deposited on graphite felt, and (d) Zn granules.

4.1 CO₂ reduction reaction

The summary of electrochemical CO₂RR experiment both of Zn Granules and Zn deposited on graphite felt as shown in Table 4, 5 respectively.

Table 4 Summary of electrochemical CO₂RR in tubular fixed-bed reactor of Zn granules

CO ₂ pressure (bar)	Voltage (V)	CO ₂ flow rate (ml min ⁻¹)	%FE _{CO}	Current (mA)	CO concentration (ppm)
1.5	8	60	4.72	40.09	245
3	8	60	6.44	91.25	755
8	8	60	10.99	82.07	1225
10	7	60	19.61	50.53	1272
10	8	60	11.42	82.41	1402
3	5	60	15.32	19.83	390
3	6	60	12.28	42.20	665
3	7	60	9.00	67.69	782
3	8	60	6.44	91.25	755
3	5	200	2.95	14.43	54
3	6	200	3.20	13.36	55
3	7	200	4.06	15.41	80
3	8	200	4.55	18.35	107

Table 5 Summary of electrochemical CO₂RR in tubular fixed-bed reactor of Zn deposited on graphite felt

CO ₂ pressure (bar)	Voltage (V)	CO ₂ flow rate (ml min ⁻¹)	%FE _{CO}	Current (mA)	CO concentration (ppm)
3	8	60	3.90	9.73	84
10	8	60	10.24	11.26	148
3	5	200	1.91	6.12	14

3	6	200	1.99	8.78	22
3	7	200	1.84	12.17	29
3	8	200	1.53	12.64	25

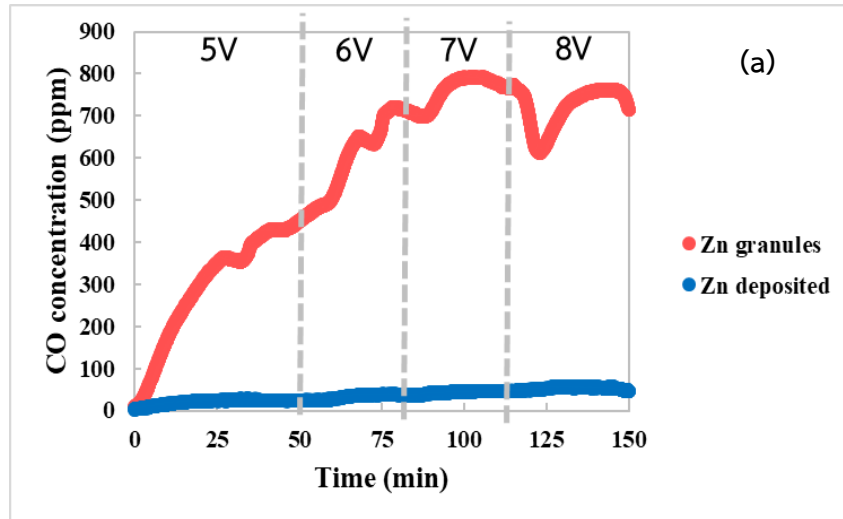
4.1.1 Voltage effect

The voltage condition used in the electrochemical tubular reactor is 5-8 V, CO₂ flow rate and pressure were controlled at 60 ml min⁻¹ and 3 bar, respectively. As a result, the highest faradaic efficiency, CO concentration, is 15.324% at 5 V and 782 ppm at 7 V.

When the applied voltage was elevated in the electrochemical CO₂ reduction reaction, the concentration of CO increased as well, which is consistent with the current that occurred. However, the higher voltage effect CO₂ on the surface of the electrode is quickly consumed, inhibiting the mass transfer limited. [26, 30]. As a result, the CO concentration at 8 V is lower than at 7 V, which occurs from producing more hydrogen evolution reaction (HER) instead of a CO₂ reduction reaction at a high applied voltage, as shown in Fig. 14, and affects decreasing the CO faradaic efficiency as shown in Fig. 15. Additionally, Zn deposited is not inhibiting the mass transfer limited due to the low-rate CO produced.

Fig. 14 and Fig. 15 can explain the Zn electrode both Zn granules and Zn deposited in electrochemical CO₂RR. From the results, CO concentration and CO faradaic efficiency of Zn granules are higher than Zn deposited which indicates the rate of CO produced in Zn deposited is low. Possibility, (1) Zn deposited to have a low quantity of Zn on graphite felt. The SEM image in fig. 13b, it shows Zn covered the graphite felt surface only, and lower current during the reaction which indicates the low active sites for CO₂ reduction [27, 28] (2) The quantity of Zn on graphite felt is not detectable after the CO₂RR experiment with Zn deposited for two hours, which influences the rate of CO production and Zn deposited is poor durability. As a

consequence, it can be said that Zn granules perform better than Zn placed at the same thickness of porous cathode.



จุฬาลงกรณ์มหาวิทยาลัย
CHULALONGKORN UNIVERSITY

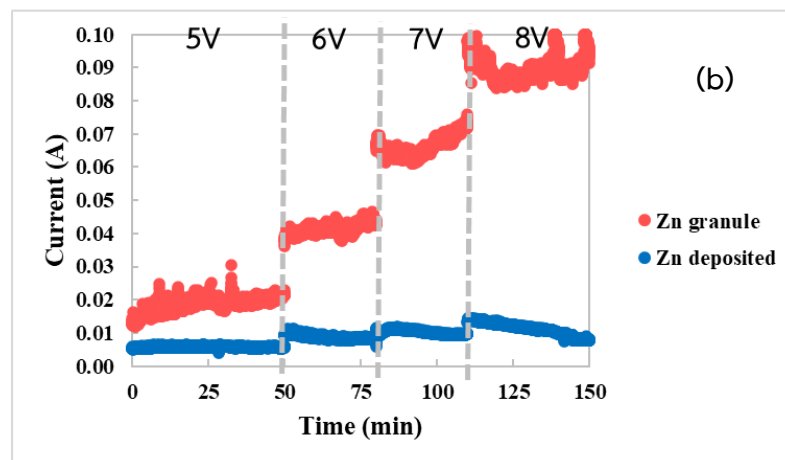


Fig. 14 (a) CO concentration (ppm), (b) current and Time (min) at 3 bar and CO₂ flow rate 60 ml min⁻¹ of Zn granules and Zn deposited.

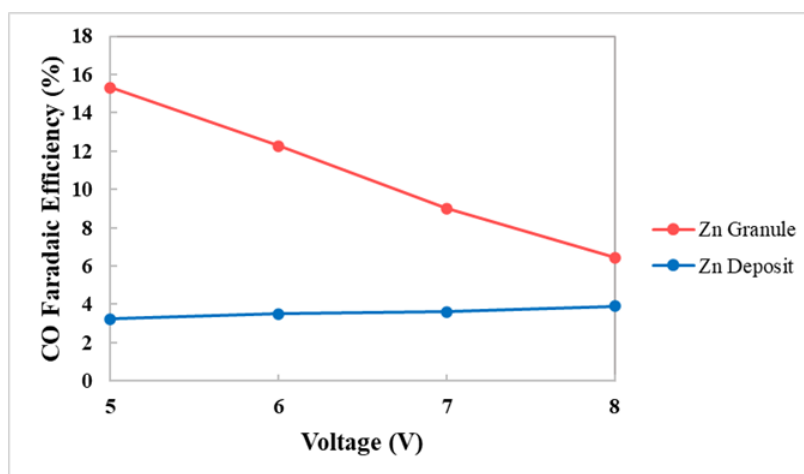


Fig. 15 CO faradaic efficiency (%) and voltage (5-8 V) at 3 bar and CO₂ flow rate 60 ml min⁻¹ of (a) Zn granules, (b) Zn deposited on graphite felt.

4.1.2 Pressure effect

The pressure condition in the electrochemical tubular reactor is 1.5, 3, 8, and 10 bar. During the experiment, the voltage and CO₂ flow rate were controlled at 5-8 V and 60 ml min⁻¹, respectively. As shown in Fig. 16, CO concentration increased from 245 ppm at 1.5 bar to 1402 ppm at 10 bar of Zn granules. From the results, when the pressure was increased, the CO concentration was enhanced in Zn granules.

Moreover, the CO faradaic efficiency calculated from experimental data, as shown in Fig. 17, increased the same as the CO concentration in both Zn granules and Zn deposited, which the CO faradaic efficiency of Zn granules increased from 6.44% (3 bar) to 11.42% (10 bar) and Zn deposited is increased from 3.9% (3 bar) to 10.24% (10 bar). For this reason, increasing the CO₂ partial pressure impacts the increased concentration of CO₂ in the electrolyte, which affects the increase in CO₂ surface coverage and reduces the number of protons adsorbed on the catalyst surface to suppress H₂ production, leading to an increase in the CO faradaic efficiency and

decreasing the current density [11, 31] that observes from the current at 10 bar lower than 3 bar in Fig. 16b.

The result can hypothesize that high pressure is enhancing help toward CO faradaic efficiency for the electrochemical tubular fixed-bed reactor. Nevertheless, this result is a preliminary study of the behavior of the system and the major competing side reaction; HER needs to be minimized for an optimal CO₂ reduction reaction.

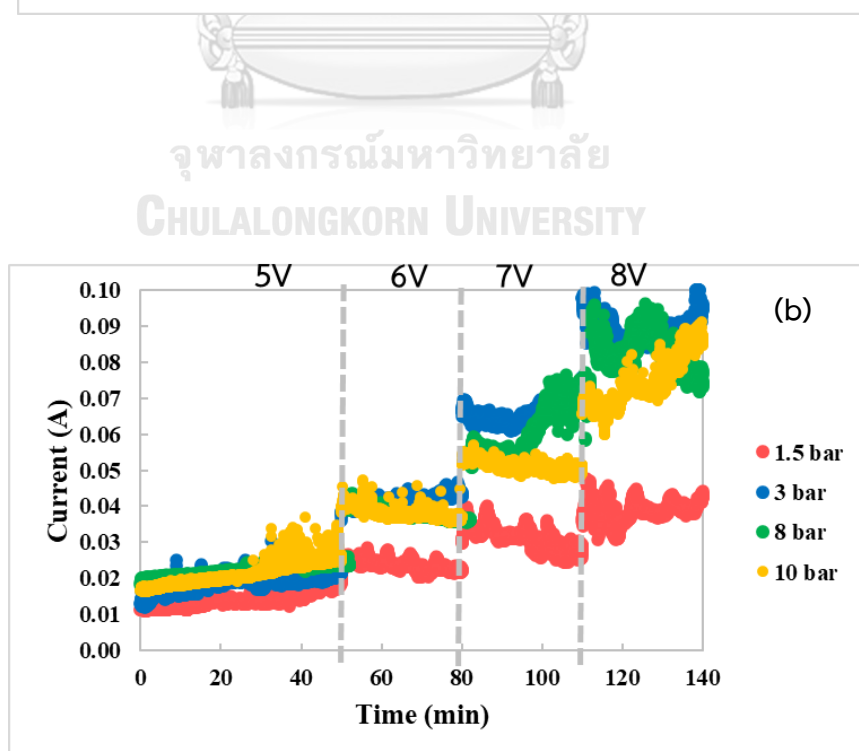
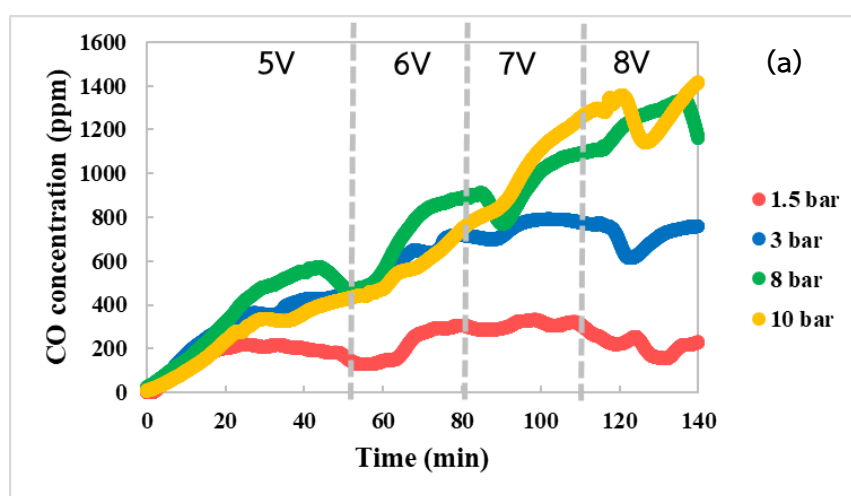


Fig. 16 (a) CO concentration (ppm), (b) Current (A) and various pressure (bar) at 8V and CO₂ flow rate 60 ml min⁻¹ of Zn granules.

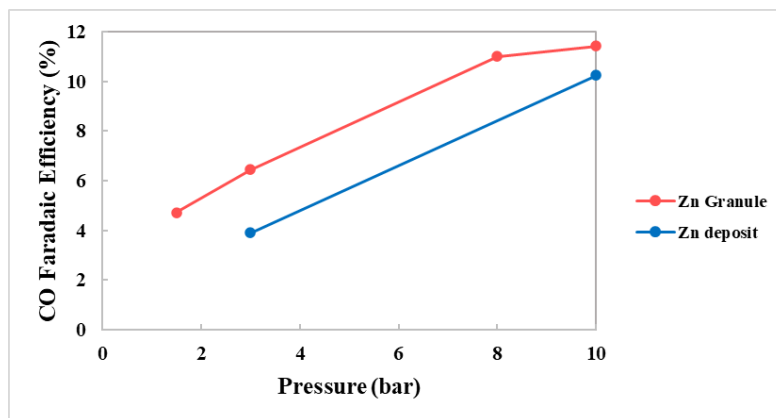


Fig. 17 CO faradaic efficiency (%) and various pressure (bar) at 8V and CO₂ flow rate 60 ml min⁻¹ of Zn granules and Zn deposited.

Fig. 18 displays the CO faradaic efficiency and current with applied various voltages from the experiment at each pressure. At 1.5 and 3 bar, the CO faradaic efficiency decreased when the voltage increased due to the over-applied voltage effect, and the highest CO faradaic efficiency was both 5 V. However, at the higher pressure (8 and 10 bar), the highest CO faradaic efficiency shifted from 5 V to 6 V (8 bar) and 7 V (10 bar) as shown in fig. 18a which operates under high-pressure conditions affects the increase of CO₂ on the surface coverage from the pressure effect causes a decrease in mass transfer limited effect of CO₂, is enough for the CO₂ reduction reaction to produce CO and it can increase the voltage for enhancing the CO faradaic efficiency. The highest CO faradaic efficiency has 19.61% at 10 bar (7 V). Furthermore, the increase of CO₂ on the surface coverage affects the decreasing H₂ formation which causes the total current is decreased. In fig. 18b, the total current for CO₂ reduction at 3 and 8 bar have higher than 10 bar.

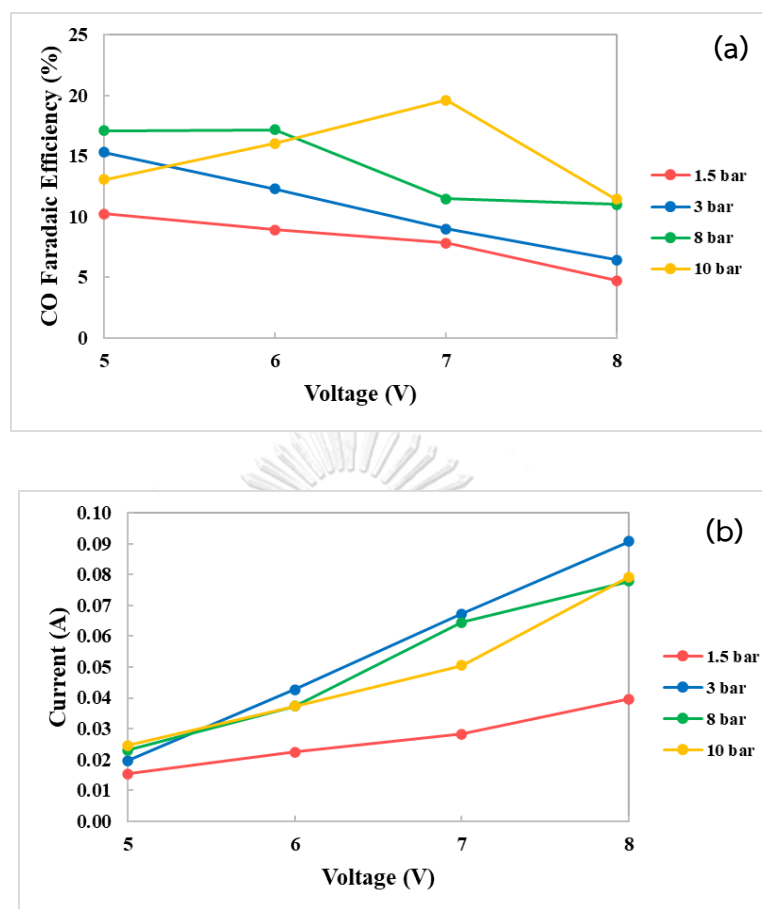


Fig. 18 (a) CO faradaic efficiency (%), (b) Current and voltage (5-8 V) at 1.5, 3, 8, 10 bar and CO₂ flow rate 60 ml min⁻¹ of Zn granules.

4.1.3 CO₂ flow rate effect

The CO₂ flow rate condition used in the electrochemical tubular reactor is 60, 200 ml min⁻¹. Voltage and pressure were controlled at 5-8 V and 3 bar, respectively. The determination of the CO faradaic efficiency is made difficult by the residence time of product gases that result in a lag in the system. So, increasing the CO₂ flow rate can solve this problem; increasing the CO₂ flow rate can reduce residence time, and the

product gases are quickly flowed into the IR analyzer and can follow the real-time result [18]. However, the higher CO₂ flow rate cause decreasing CO concentration as shown in fig.19, the CO concentration decreased from ~800 ppm (60 ml min⁻¹) to ~100 ppm (200 ml min⁻¹) because a higher CO₂ flow rate effected to decreases the contact time between catalyst and reactant, leading to a decrease in CO production and CO faradaic efficiency in the system.

As illustrated in fig. 20 of Zn granules at 60 ml min⁻¹, the CO₂ reduction process has mass transfers limited at a higher voltage. The higher CO₂ flow rate has no effect on mass transfers at 200 ml min⁻¹ because the increasing CO₂ flow rate reduces CO production and the amount of CO₂ on the surface is sufficient for the CO₂ reduction.

The CO₂ flow rate effect of Zn deposited on graphite felt at 60-200 ml min⁻¹, both CO concentration and current have slightly difference which concludes the flow rate is not effective for the CO concentration and CO faradaic efficiency. So, Using Zn deposited in electrochemical CO₂RR in a tubular reactor suggests a higher flow rate for reducing lag in the system, which can follow the real-time product gases.

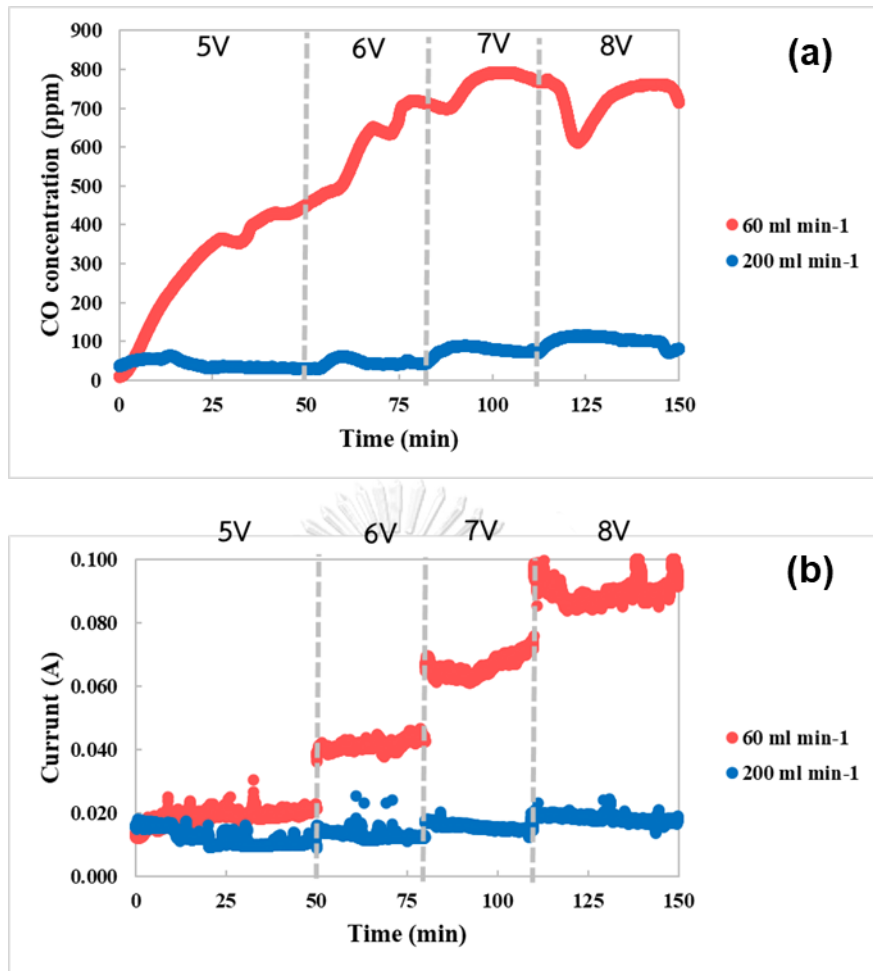


Fig. 19 (a) CO concentration, (b) Current of various CO₂ flow rate (60, 200 ml min⁻¹) and Voltage (5-8 V) at 3 bar of Zn granules

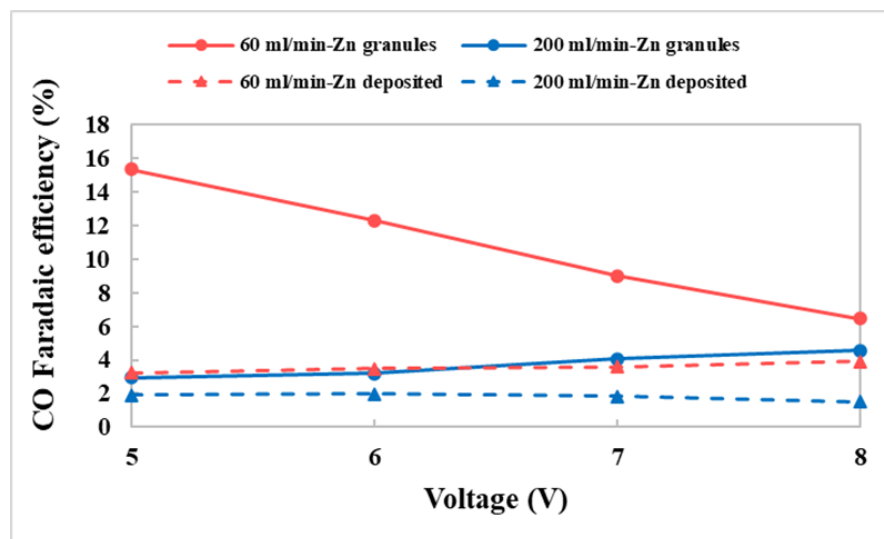
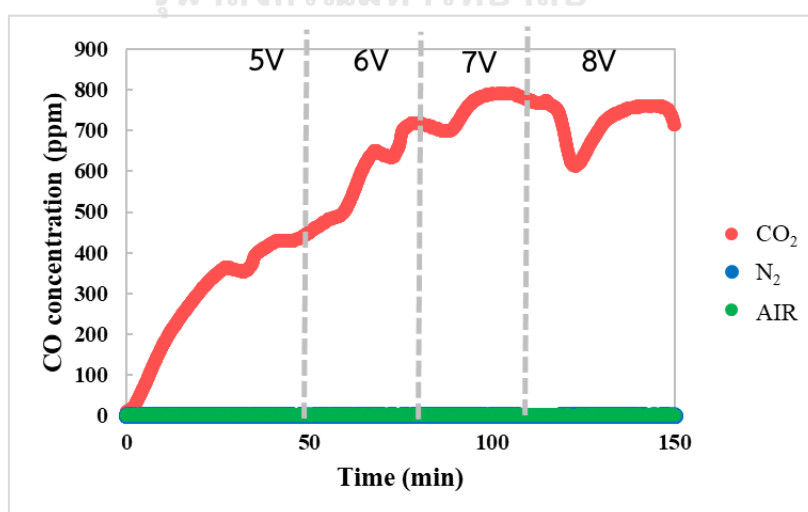


Fig. 20 CO faradaic efficiency of various CO₂ flow rate (60, 200 ml min⁻¹) and Time (min) at 3 bar of Zn granules

4.2 Blank Test

From the results, the behavior of electrochemical CO₂RR for CO₂ to CO production for confirming CO products is produced with CO₂RR by feed N₂ replacing the saturated CO₂ gas. The result is shown in Fig. 21a; the amount of CO detected with Infrared Gas Analyzer (IR) was negligible compared with CO₂RR at 3 bar, 5-8 V, 60 ml min⁻¹, resulting indicates the CO production was produced via saturated CO₂. The current of feed N₂ is lower than the CO₂RR, which is OER current from only water splitting.

For scale-up in the electrochemical tubular fixed-bed can be a series. Therefore, the possibility of reducing O₂ gas in the next cell decreases the CO faradaic efficiency and CO concentration in the system by feeding Air into the system instead of the saturated CO₂ gas. In Fig. 21b, the current of Air is 1/3 or 1/4 times of CO₂ reduction, indicating the O₂ gas is reduced. Thus, the scale-up the electrochemical tubular fixed-bed must be considering the O₂ gas again.



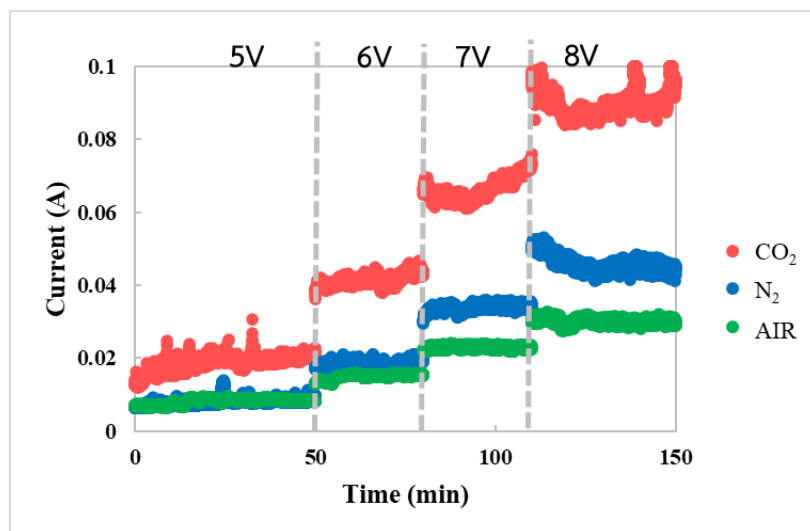


Fig. 21 (a) CO concentration (ppm), (b) Current (A) of blank test comparing at 3 bar, 5-8 V, 60 ml min⁻¹ and Time (min)



5.1 Conclusions

Electrochemical CO₂RR is usually studied in the liquid phase by electrolyte solution with saturated CO₂ in conventional H-type cells. However, the solubility of CO₂ is low at room temperature and atmospheric pressure leads to mass transfer limitations. So, the development of type cells from H-cell become to tubular is a good

choice for solving this problem because the tubular reactor can carry out at high pressure.

The Electrochemical tubular reactor was studied at high pressure, voltage, and CO₂ flow rate. As soon as increase the pressure, the CO concentration and faradaic efficiency rise. At 10 bar, the highest CO faradaic efficiency of 19.61%. Moreover, at the high-pressure exhibits increase CO faradaic efficiency, CO concentration at higher voltage. The applied voltage suggested for the electrochemical tubular reactor is around 5 V. The effect of the CO₂ flow rate is an essential parameter for reducing the lag time that happens in the system. Nevertheless, the CO₂ flow rate leads to low CO faradaic efficiency same.

The behavior of CO production was observed by N₂ gas, indicate the CO gas occurred with Electrochemical CO₂ reduction reaction on cathode by saturated CO₂ and the behavior O₂ gas for the future CO₂ reduction reaction cell, cannot reduced on the cathode.

5.2 Suggestions

- The thickness of the ion-exchange resin bead can be improved to reduce the resistance for the scale-up part of the electrochemical tubular fixed-bed reactor.
- The other product gas and liquid product are produced in the electrochemical CO₂RR should be detect to analyze and study the behavior of cell.

REFERENCES

1. Tufa, R.A., et al., *Towards highly efficient electrochemical CO₂ reduction: Cell designs, membranes and electrocatalysts*. Applied Energy, 2020. **277**.
2. Jin, S., et al., *Advances and Challenges for the Electrochemical Reduction of CO₂ to CO: From Fundamentals to Industrialization*. Angew Chem Int Ed Engl, 2021. **60**(38): p. 20627-20648.
3. Lin, R., et al., *Electrochemical Reactors for CO₂ Conversion*. Catalysts, 2020. **10**(5).
4. Jhong, H.-R.M., S. Ma, and P.J.A. Kenis, *Electrochemical conversion of CO₂ to useful chemicals: current status, remaining challenges, and future opportunities*. Current Opinion in Chemical Engineering, 2013. **2**(2): p. 191-199.
5. Wang, G., et al., *Electrocatalysis for CO₂ conversion: from fundamentals to value-added products*. Chem Soc Rev, 2021. **50**(8): p. 4993-5061.
6. Proietto, F., et al., *Electrochemical conversion of pressurized CO₂ at simple silver-based cathodes in undivided cells: study of the effect of pressure and other operative parameters*. Journal of Applied Electrochemistry, 2020. **51**(2): p. 267-282.
7. Qin, B., et al., *Electrochemical Reduction of CO₂ into Tunable Syngas Production by Regulating the Crystal Facets of Earth-Abundant Zn Catalyst*. ACS Appl Mater Interfaces, 2018. **10**(24): p. 20530-20539.
8. Ham, Y.S., et al., *Proton-exchange membrane CO₂ electrolyzer for CO production using Ag catalyst directly electrodeposited onto gas diffusion layer*. Journal of Power Sources, 2019. **437**.
9. Liang, S., et al., *Electrolytic cell design for electrochemical CO₂ reduction*. Journal of CO₂ Utilization, 2020. **35**: p. 90-105.
10. Zhang, X., et al., *Electrocatalytic carbon dioxide reduction: from fundamental principles to catalyst design*. Materials Today Advances, 2020. **7**.

11. Garg, S., et al., *Advances and challenges in electrochemical CO₂ reduction processes: an engineering and design perspective looking beyond new catalyst materials*. Journal of Materials Chemistry A, 2020. **8**(4): p. 1511-1544.
12. Lu, Q. and F. Jiao, *Electrochemical CO₂ reduction: Electrocatalyst, reaction mechanism, and process engineering*. Nano Energy, 2016. **29**: p. 439-456.
13. Gamburg, Y.D., & Zangari, G., *Theory and practice of metal electrodeposition*. 2011.
14. Küngas, R., *Review—Electrochemical CO₂ Reduction for CO Production: Comparison of Low- and High-Temperature Electrolysis Technologies*. Journal of The Electrochemical Society, 2020. **167**(4): p. 044508.
15. Dickinson, E.J.F. and A.J. Wain, *The Butler-Volmer equation in electrochemical theory: Origins, value, and practical application*. Journal of Electroanalytical Chemistry, 2020. **872**: p. 114145.
16. Lee, J., et al., *Electrochemical CO₂ reduction using alkaline membrane electrode assembly on various metal electrodes*. Journal of CO₂ Utilization, 2019. **31**: p. 244-250.
17. Luo, W., et al., *Boosting CO Production in Electrocatalytic CO₂ Reduction on Highly Porous Zn Catalysts*. ACS Catalysis, 2019. **9**(5): p. 3783-3791.
18. Dufek, E.J., et al., *Operation of a Pressurized System for Continuous Reduction of CO₂*. Journal of The Electrochemical Society, 2012. **159**(9): p. F514-F517.
19. Hori, Y., et al., *Electrocatalytic process of CO selectivity in electrochemical reduction of CO₂ at metal electrodes in aqueous media*. Electrochimica Acta, 1994. **39**(11): p. 1833-1839.
20. Tufa, R.A., et al., *Towards highly efficient electrochemical CO₂ reduction: Cell designs, membranes and electrocatalysts*. Applied Energy, 2020. **277**: p. 115557.
21. Ramdin, M., et al., *High Pressure Electrochemical Reduction of CO₂ to Formic Acid/Formate: A Comparison between Bipolar Membranes and Cation Exchange Membranes*. Industrial & Engineering Chemistry Research, 2019. **58**(5): p. 1834-1847.

22. Kohjiro, H., K. Akihiko, and S. Tadayoshi, *Electrochemical reduction of carbon dioxide under high pressure on various electrodes in an aqueous electrolyte*. J Electronal Chem, 1995: p. 141-147.
23. Gabardo, C.M., et al., *Combined high alkalinity and pressurization enable efficient CO₂ electroreduction to CO*. Energy & Environmental Science, 2018. **11**(9): p. 2531-2539.
24. Messias, S., et al., *Electrochemical production of syngas from CO₂ at pressures up to 30 bar in electrolytes containing ionic liquid*. Reaction Chemistry & Engineering, 2019. **4**(11): p. 1982-1990.
25. Yuliy D. Gamburg, G.Z., *Introduction to electrodeposition: Basic terms and fundamental concepts, Electrodeposition of Zinc and Its Alloys, in Theory and Practice of Metal Electrodeposition*, G.Z. Yuliy D. Gamburg, Editor. 2011, Springer New York, NY. p. 1-25, 284-290.
26. Lu, Y., et al., *Efficient electrocatalytic reduction of CO₂ to CO on an electrodeposited Zn porous network*. Electrochemistry Communications, 2018. **97**: p. 87-90.
27. Rosen, J., et al., *Electrodeposited Zn Dendrites with Enhanced CO Selectivity for Electrocatalytic CO₂ Reduction*. ACS Catalysis, 2015. **5**(8): p. 4586-4591.
28. Won da, H., et al., *Highly Efficient, Selective, and Stable CO₂ Electroreduction on a Hexagonal Zn Catalyst*. Angew Chem Int Ed Engl, 2016. **55**(32): p. 9297-300.
29. Luo, W., et al., *Electrochemical reconstruction of ZnO for selective reduction of CO₂ to CO*. Applied Catalysis B: Environmental, 2020. **273**.
30. Jiang, X., et al., *Electrocatalytic reduction of carbon dioxide over reduced nanoporous zinc oxide*. Electrochemistry Communications, 2016. **68**: p. 67-70.
31. Hori, Y., A. Murata, and Y. Yoshinami, *Adsorption of CO, intermediately formed in electrochemical reduction of CO₂, at a copper electrode*. Journal of the Chemical Society, Faraday Transactions, 1991. **87**(1): p. 125.



จุฬาลงกรณ์มหาวิทยาลัย
CHULALONGKORN UNIVERSITY



จุฬาลงกรณ์มหาวิทยาลัย
CHULALONGKORN UNIVERSITY

VITA

NAME Pakawat Sengchim

DATE OF BIRTH 26 December 1997

PLACE OF BIRTH Songkhla

INSTITUTIONS ATTENDED Faculty of engineering, Chemical engineering department
Prince of Songkla University
Bachelor of Engineering (B.Eng.)

HOME ADDRESS 124, Moo.3, Khlong Hoi Khong, Songkhla, 90230

